THE AMERICAN SOCIETY OF MECHANICAL ENGINEERS
345 E. 47th St., New York, N.Y. 10017

98-GT-549

GENERATION OF FIVE-AXIS CUTTER PATHS FOR A BALL-END CUTTER WITH GLOBAL INTERFERENCE CHECKING

Der Min Tsay and Wei Feng Yan

Department of Mechanical Engineering
National Sun Yat-Sen University
Kaohsiung, TAIWAN R.O.C.

(Phone: 886-7-525-4229 Fax:886-7-525-4299 Email:dermin@mail.nsysu.edu.tw)

ABSTRACT

A simple, yet useful procedure is developed to generate tool paths with global interference checking for five-axis machining of turbomachinery components with complex geometries. Based on the projected distance between the surface data and the cutter-axis of a cylindrical ball-end mill, interference between the surface of a workpiece and the cutter can be detected. Given the cutter contact points of the surface and the cutter's size, it can produce the cutter location data without incurring interference through relatively rotating and tilting the workpiece. Applications of the developed approach to five-axis machining of centrifugal compressor impellers with thirteen and fifteen blades are illustrated to demonstrate the usefulness and reliability of the procedure.

INTRODUCTION

To efficiently machine turbomachinery components such as centrifugal compressors, axial compressors, and fans having complex, overlapping surface geometries, five-axis numerically controlled (NC) machine tools possessing many degrees of freedom are necessarily utilized. To produce such components with desired precision, correct cutter contact (CC) data must first be generated considering the scallop height (Kim and Chu, 1994; Tsay and Hwang, 1994), overcutting, and local gouging (Oliver et al., 1993) of the part surfaces. More importantly, before machining, the possibility of tool interference must be avoided so that proper cutter location (CL) data can be decided and tool paths can be schemed. Otherwise, desired geometries of parts may be cut and/or the impact may result in the fracture of the cutter and the damage of the machine tool.

To machine parametric, sculptured surfaces within specified tolerances, a number of studies have been reported to characterize the scallop height and/or to improve it for local gouging. Loney and Ozsoy (1987) proposed a numerical procedure to find the parametric value that will produce the largest chordal deviation. Vickers and Quan (1989) determined the effective radius of a flat-end cutter as a function of cutter-tilting angles for machining low curvature surfaces. By establishing triangular polyhedron models (Choi and Jun, 1989; Hwang, 1992), CL data without gouging can be yielded by checking the distances from the center of the ball-end mill to the CC data along tool paths. Oliver et al. (1993) developed two techniques to analyze the chordal deviation and to detect gouging. By five-axis surface machining, Choi et al. (1993) generated CL data from the given CC paths to give minimum cusp heights. Also, based on the chordal deviation and the scallop height, the surface roughness was analyzed in the machining process (Tsay and Hwang, 1994). Recently, based on the constant scallop height, Suresh and Yang (1994) represented a method to generate the tool paths. In order to remove the collision problem between the cutter and the workpiece, various approaches have been attempted to deal with global cutter interference. Typically, constructing solid models, Wang (1990) proposed an algorithm to calculate interference-free zones utilizing a moving frame of reference. Using recursive subdivision of the control polygon of Bezier curves and surfaces, Tseng and Joshi (1991) showed algorithms to determine tool-approach directions without interference. Based on the solid modeling technique, Takeuchi and Idemura (1991) as well as Takeuchi and Watanabe (1992) generated collision-free tool paths by checking the shape data of the tool that is never within the workpiece. Also, employing the control polygon of a sculptured surface, Lee (1993) developed a procedure to find the feasible cutter orientation range without collision. Approximating surfaces into a set of polygons, Li and Jerard (1994) recently used a bucketing scheme (Jerard et al., 1989) to detect interference between a flat-end cutter and a polygon, and adjusted the tool-axis to avoid it.

To successfully machine turbomachinery components, the procedure described here provides a relatively simple and useful tool to produce cutter paths with global tool interference checking. Usually the complete geometry of a turbomachinery component is composed of various types of surfaces, i.e., blending surfaces, ruled surfaces, and sculptured surfaces. Regardless of the type of surfaces, in this article to detect global interference, it is more convenient to select CC points for checking. Furthermore, as mentioned earlier, the number of CC points can also be determined according to the analysis of surface

Presented at the International Gas Turbine & Aeroengine Congress & Exhibition
Stockholm, Sweden — June 2–June 5, 1998

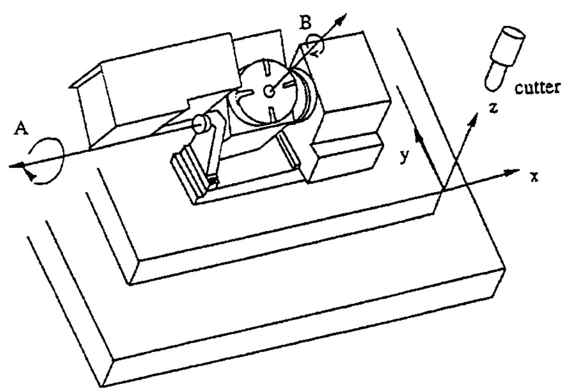

Fig. 1 Schematic illustration of a type of five-axis machining

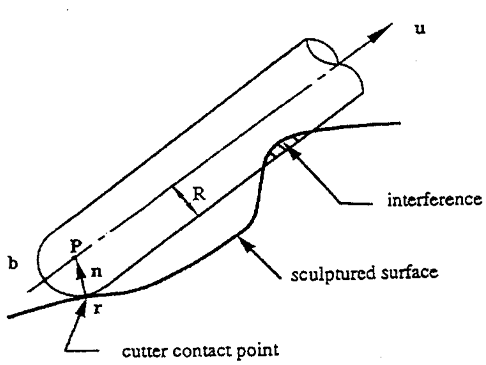

Fig. 2 Schematic illustration of interference and cutter location

roughness for manufacturing tolerances. Based on the projected distance between the CC point and the cutter-axis as well as the size of a cylindrical ball-end mill, interference between the desired surface and the cutter can be detected. As a result, admissible tool rotating and tilting ranges can be determined. Therefore, the CL data required in the machining process can be generated through rotating and tilting the workpiece. For the sake of convenience, the steps needed to fulfill the approach will be outlined based on a popular type of five-axis machining shown in Fig. 1. By the use of this method, practical application examples for machining compressor impellers by the type of a five-axis machining center is given to illustrate its effectiveness and reliability.

BACKGROUND

As shown in Fig. 2, during the machining process, the cutter is guided to touch a prescribed CC point, **r**, on the surface of a workpiece. With an offset equal to the radius, *R*, of the cylindrical ball-end cutter, the offset point of **r** can be denoted as $\mathbf{p} = \mathbf{r} + R\mathbf{n}$. **n** is the unit normal

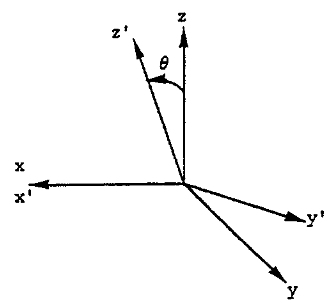

Fig. 3 Coordinate systems

vector at point **r**, and it can be easily evaluated for a general parametric surface (Faux and Pratt, 1979). Corresponding to **r**, the CL data, $\mathbf{L} = (\mathbf{b},\mathbf{u})$, can be expressed by the position of the tip of the cutter, **b**, and the unit vector of the cutter-axis. Note that **b** can be written as

$$\mathbf{b} = \mathbf{r} + R(\mathbf{n} - \mathbf{u}) \tag{1}$$

The global interference problem is defined as any portion of the desired geometry of a workpiece is within the flank of a cylindrical ball-end cutter. To overcome this difficulty, by rotating and tilting the rotary table of the machining center plotted in Fig. 1, the direction of the tool axis can be relatively adjusted so that a new vector of **u** needed in Eq. (1) can be evaluated. As a result, a CL data without interference may be found from Eq. (1).

In order to find an admissible direction of the cutter-axis without interference, based on the configuration of a five-axis machine tool illustrated in Fig. 1, the coordinates of a CC point on the workpiece is first rotated about the z-axis for an angle of ϕ and then tilted about the x-axis for an angle of θ in the x-y-z coordinate system shown in Fig. 3. In this sequence, the involved process of calculations for finding an admissible direction of the cutter-axis will be more convenient. This process of transformation can be written in a matrix form as

$$[R_{zx}] = [R_z \phi][R_x \theta] \tag{2}$$

The result above is also identical to that obtained by tilting the workpiece for an angle of θ about the x-axis and then rotating it about the z'-axis in the x'-y'-z' coordinate system illustrated in Fig. 3 for an angle of ϕ. In operation of the rotary table plotted in Fig. 1, note that the rotation (B-axis) is performed about the z'-axis whose direction is changed due to a tilt of θ about the x-axis. The transformation matrix of this step can be expressed as

$$[R_{xz'}] = [R_x \theta][R_{z'} \phi] \tag{3}$$

The identity between Eqs. (2) and (3) is established in the following paragraphs. The well-known complete transformation for a general case of rotation about an arbitrary axis in space can be described as (Rogers and Adams, 1990, pp. 123)

$$[M] = [T][R_X][R_y][R_\phi][R_y]^{-1}[R_X]^{-1}[T]^{-1} \tag{4}$$

where $[T]$, $[R_X]$, and $[R_y]$ respectively denote the translation matrix, the transformation matrix for rotation about the x-axis, and the transformation matrix for rotation about the y-axis. And, $[R_\phi]$ is a z-axis rotation matrix for the rotation about the arbitrary axis. Others in the right-hand side of Eq. (4) are inverse matrices. By referring to Fig. 3, since the z'-axis passes through the origin, the transformation for a rotation about the z'-axis is relatively simple and can be written as

$$[R_{z'}\phi] = [M_{z'}\phi] = [R_X][R_\phi][R_X]^{-1} \tag{5}$$

To make the z'-axis coincident with the z-axis, it is necessary to rotate an angle of $-\theta$ about the x-axis and the transformation matrix, $[R_X]$, is

$$[R_X] = [R_X(-\theta)] = \begin{bmatrix} 1 & 0 & 0 & 0 \\ 0 & \cos(-\theta) & \sin(-\theta) & 0 \\ 0 & -\sin(-\theta) & \cos(-\theta) & 0 \\ 0 & 0 & 0 & 1 \end{bmatrix}$$

$$= \begin{bmatrix} 1 & 0 & 0 & 0 \\ 0 & \cos\theta & \sin\theta & 0 \\ 0 & -\sin\theta & \cos\theta & 0 \\ 0 & 0 & 0 & 1 \end{bmatrix}^{-1} = [R_X\theta]^{-1} \tag{6}$$

The rotation matrix, $[R_\phi]$, is performed for an angle of ϕ about the z-axis, and it can be denoted as $[R_\phi] = [R_Z\phi]$. Also, note that

$$[R_X]^{-1} = [R_X(-\theta)]^{-1}$$

$$= \begin{bmatrix} 1 & 0 & 0 & 0 \\ 0 & \cos(-\theta) & \sin(-\theta) & 0 \\ 0 & -\sin(-\theta) & \cos(-\theta) & 0 \\ 0 & 0 & 0 & 1 \end{bmatrix}^{-1} = [R_X\theta] \tag{7}$$

Therefore, Eq. (5) can be expressed as

$$[R_{Z'}\phi] = [R_X(-\theta)][R_Z\phi][R_X(-\theta)]^{-1} = [R_X\theta]^{-1}[R_Z\phi][R_X\theta] \tag{8}$$

From Eq. (8), one can see that the result of Eq. (2) coincides with that of Eq. (3) because

$$[R_{XZ'}] = [R_X\theta][R_{Z'}\phi] = [R_X\theta][R_X\theta]^{-1}[R_Z\phi][R_X\theta]$$
$$= [R_Z\phi][R_X\theta] = [R_{ZX}] \tag{9}$$

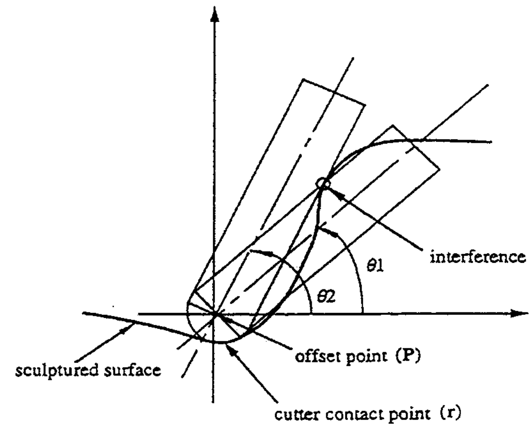

Fig. 4 Schematic illustration of rotational range of a cutter and interference

DETERMINATION OF ADMISSIBLE CUTTER ORIENTATION

As described earlier, the task of machining turbomachinery components with complex geometries can be conveniently accomplished by using five-axis machine tools especially when the global interference problem is to be overcome. In preparation for producing tool paths, the center of the ball-end of a cutter with a specified orientation is placed at the offset point of a CC point with an offset equal to the radius of the cutter. Then, as depicted in Fig. 4, the CC point is checked for interference between the workpiece and the cutter. To create interference-free cutter paths by adjusting tilting and rotating axes of a five-axis machine tool, all the schemed CC points must be outside of the flank of the cutter.

Given CC points and based on the projected distance between the CC point and the axis of a cylindrical cutter to detect interference, the procedure to generate interference-free tool paths is described in a step-wise fashion in the following outlines:

(1) Select an appropriate size of a cylindrical cutter with a ball-end, considering the geometric features of a workpiece;

(2) Calculate the offset point mentioned earlier for each CC point. And, then position the center of the ball-end of the cutter at the offset point by moving the three translation axes of the five-axis machine tool;

(3) Choose a proper angle of ϕ for turning the B-axis of the machine tool indicated in Fig. 1. The angle also depends upon the geometric features of a particular workpiece and the selected size of the mill;

(4) Calculate the angular range of θ for the A-axis shown in Fig. 1, based on the angle of ϕ determined in the step above;

(4-1) Compute the possible angular range of a CC point by rotating the cutter (flank) about the offset point to touch all other CC points that are assumed to be interference points illustrated in Fig. 4;

(4-2) Find the intersection of angular ranges determined above. The common range will constitute the possible tilting range for the single CC point;

(4-3) Decide a tilting angle by avoiding the direction of the axis of the ball-end cutter being collinear to that of the CC point normal;

(4-4) Generate the CL data for the CC point based on the angles of ϕ and θ;

(5) Repeat steps of (4-1) through (4-4) for all CC points.

The CL data obtained above are applicable to a simultaneous five-axis machine tool without incurring collision. If the motion control of a five-axis machine tool is not simultaneous for its rotary table, one more step is required to find the intersection of ranges for tilting angles corresponding to the CC points along a schemed tool path. Then, a specific tilting angle decided from the intersection of tilting ranges for a single tool path may be used with such a machine tool.

The steps described above can be easily implemented to obtain the admissible direction of the cutter-axis without incurring interference by rotating and tilting the workpiece. The calculations and solution needed in step (4-1) above for a CC point will be illustrated in detail below for two types of five-axis machine tools.

Referring to Fig. 1, for a point, (x, y, z), in space, one selects an angle of ϕ for rotation about the z-axis and this transformation can be expressed as

$$(x', y', z') = (x, y, z)\begin{bmatrix} \cos\phi & \sin\phi & 0 \\ -\sin\phi & \cos\phi & 0 \\ 0 & 0 & 1 \end{bmatrix}$$
$$= (x\cos\phi - y\sin\phi, x\sin\phi + y\cos\phi, z) \quad (10)$$

Then, the transformation of the point in Eq. (10) tilted about the x-axis for an angle of θ can be written as

$$(x'', y'', z'') = (x', y', z')\begin{bmatrix} 1 & 0 & 0 \\ 0 & \cos\theta & \sin\theta \\ 0 & -\sin\theta & \cos\theta \end{bmatrix}$$
$$= (x', y'\cos\theta - z'\sin\theta, y'\sin\theta + z'\cos\theta) \quad (11)$$

From the result of the coordinate transformation given in Eq. (11), if a CC point just touches the flank of a cutter, then the projected distance from the CC point to the offset point, i.e., center of the cylindrical ball-end of the cutter, is equal to the radius of the mill and can be shown as

$$(x''_{cc} - x''_{of})^2 + (y''_{cc} - y''_{of})^2 = R^2 \quad (12)$$

where subscripts, cc and of, respectively denote coordinates of the CC point and the offset point. Eq. (12) can be further described as

$$[(y'_{cc} - y'_{of})\cos\theta - (z'_{cc} - z'_{of})\sin\theta]^2 = R^2 - (x'_{cc} - x'_{of})^2 \quad (13)$$

Substituting $b = y'_{cc} - y'_{of}$, $c = z'_{cc} - z'_{of}$, and $a = R^2 - (x'_{cc} - x'_{of})$ into Eq. (13) yields

$$(b\cos\theta - c\sin\theta)^2 = a \quad (14)$$

Using trigonometric relationships, one can also write Eq. (14) as

$$b^2(\frac{1+\cos 2\theta}{2}) + c^2(\frac{1-\cos 2\theta}{2}) + 2bc\cos\theta\sin\theta = a \quad (15)$$

Moreover, Eq. (15) can be represented as

$$e\cos 2\theta + f\sin 2\theta = g \quad (16)$$

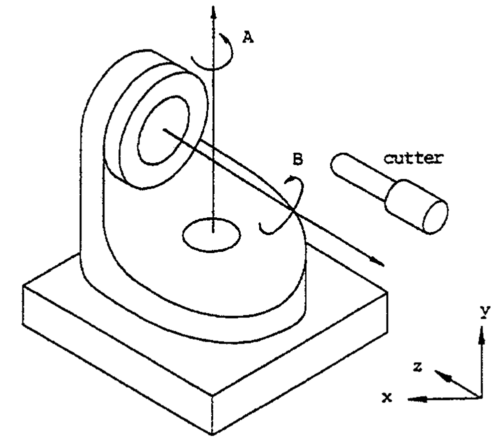

Fig. 5 Schematic illustration of a different type of five-axis machining

where $e = \frac{b^2 - c^2}{2}$, $f = bc$, and $g = a - (\frac{b^2 + c^2}{2})$

Letting $\tan\theta = t$ and substituting $\sin 2\theta = \frac{2t}{1+t^2}$ as well as $\cos 2\theta = \frac{1-t^2}{1+t^2}$ into Eq. (16), one can derive the solution of Eq. (16) as

$$t_{1,2} = \frac{f \pm \sqrt{f^2 - (g^2 - e^2)}}{(g+e)} \quad (17)$$

or

$$\theta_{1,2} = \tan^{-1}(t_{1,2}) \quad (18)$$

Note that Eq. (18) shows that two roots for the admissible tilting range of a CC point are obtained and illustrated in Fig. 4. As described earlier, tilting ranges for other CC points can be solved in a similar way.

Based on a different type of five-axis machining shown in Fig. 5, the derivation of the tilting range for a CC point is given here. Comparing the configuration of this machine to that shown in Fig. 1, one can see that the A-axis of this machine is tilted about the y-axis and the B-axis is rotated about the z-axis. Therefore, one can modify Eq. (11) as

$$(x'', y'', z'') = (x', y', z')\begin{bmatrix} \cos\theta & 0 & -\sin\theta \\ 0 & 1 & 0 \\ \sin\theta & 0 & \cos\theta \end{bmatrix}$$
$$= (x'\cos\theta + z'\sin\theta, y', -x'\sin\theta + z'\cos\theta) \quad (19)$$

In a similar manner, if a CC point just touches the flank of the cutter, then the projected distance, Eq. (12), from the CC point to the offset point can be written as

$$[(x'_{cc}\cos\theta + z'_{cc}\sin\theta) - (x'_{of}\cos\theta + z'_{of}\sin\theta)]^2 + (y'_{cc} - y'_{of})^2 = R^2 \quad (20)$$

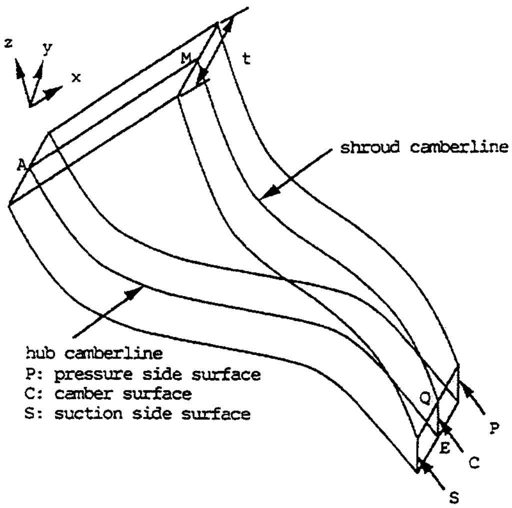

Fig. 6 Schematic illustration of camber, pressure side, and suction side surfaces of an impeller

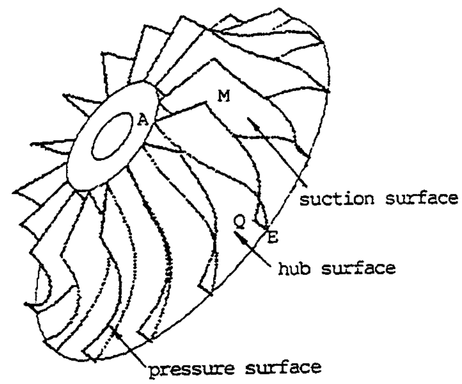

Fig. 7 Schematic illustration of a fifteen-blade impeller

Letting $b = x'_{cc} - x'_{of}$, $c = z'_{cc} - z'_{of}$, and $a = R^2 - (y'_{cc} - y'_{of})^2$, one can express Eq. (20) as

$$(b\cos\theta - c\sin\theta)^2 = a \tag{21}$$

It is obvious that the formula above has the same form as that of Eq. (14). Hence, for a five-axis machine tool of this type, the same solution given in Eq. (18) can be again employed in the process of finding the admissible tilting range for a CC point.

APPLICATION EXAMPLES

To verify the usefulness and reliability of the approach described above, machining of various sizes and designs of centrifugal compressor impellers having thirteen and fifteen blades is demonstrated. To ensure that impellers will stably operate to meet design requirements, they must be accurately machined. Because the geometries of such turbomachinery components are very complicated and the degree of potential interference during cutting is very high, it is necessary to scheme the appropriate interference-free tool paths for five-axis machining.

Before performing the procedure here, the basic definitions about the geometry of impellers must first be introduced. The geometry of an impeller is basically characterized by its blade and hub surfaces. Represented by ruled surfaces (Rogers and Adams, 1990), a blade is defined by a camber surface (Smith and Merryweather, 1973). It is used to form the pressure side surface and the suction side surface by the offset surfaces of the camber surface with an offset from both sides (Smith and Merryweather, 1973). As indicated in Fig. 6, a camber surface is a ruled surface constructed by linearly interpolating between two known boundary curves, the hub camberline (curve A-E) and the shroud camberline (curve M-Q). Therefore, the pressure side and suction side surfaces are also ruled surfaces. By referring to Fig. 7, the hub surface is generated by rotating the hub camberline with respect to the axis of the impeller. In addition, a constant-radius blending technique (Choi, 1991) is applied to construct the blends between the blade and the hub regions for pressure and suction sides.

Based on the necessary steps mentioned earlier to generate collision-free tool paths for cutting an impeller with fifteen blades illustrated in Fig. 7, an interactive computer code in C language is developed and run on a personal computer to implement the procedure. The size of the blank of the impeller in this application is 118 mm and 36 mm for its diameter and height, respectively. The minimal gap between two neighboring blades of this fifteen-blade impeller is below 9 mm. The diameter of the chosen cylindrical ball-end cutter is 4 mm.

With the consideration of the gap between two neighboring blades of the impeller and the size of the mill, the angle of $\phi = 12^0$ is selected for calculations. For checking collision, the numbers of CC points in each block between two neighboring blades for the pressure side surface, the suction side surface, and the hub surface are determined based on the analysis of surface roughness (Tsay and Hwang, 1994) for manufacturing tolerances. The resulting CL data are further postprocessed for employing the type of five-axis machining shown in Fig. 1 to machine the impeller.

As mentioned earlier, for a CC point, a range for the tilting angles without incurring interference may be identified even though it is limited within a small zone. In order to select a tilting angle for each CC point for cutting the impeller, the orientation of the cutter-axis can further be checked. Since the tip of a cylindrical ball-end cutter has the lowest efficiency in material-removal rates, if possible, the direction of the cutter-axis should not be collinear to that of the CC point normal. Otherwise, as presented in Fig. 8 with the simulated result and the cut impeller, the tip of the cutter will often leave tool marks on the hub surface of the impeller. Improvement for this situation is reflected in Fig. 9 with the simulated result and the cut impeller. Fig. 10 shows the complete geometry of the successfully cut impeller.

In a similar way, Fig. 11 illustrates the five-axis machining of an impeller with thirteen blades by the use of the proposed method for generating interference-free tool paths. The machined impeller is photographed in Fig. 12.

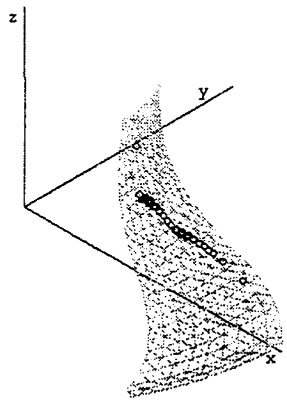

(a)

(b)

Fig. 8 (a) Simulated result for tool marks (b) Tool marks left on the cut hub surface

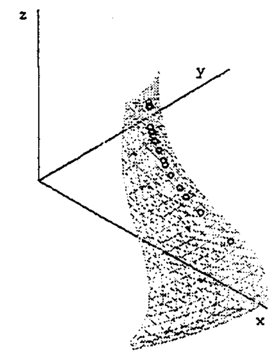

(a)

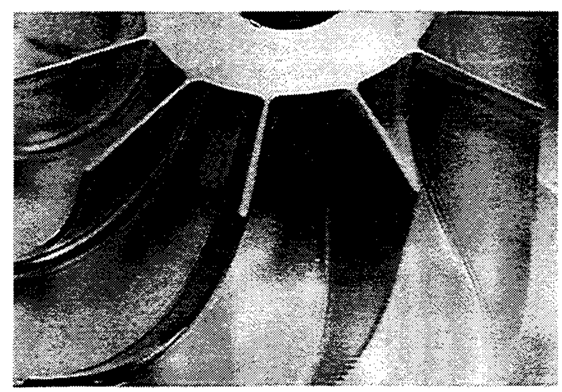

(b)

Fig. 9 (a) Simulated result for improved tool marks (b) Improved tool marks left on the cut hub surface

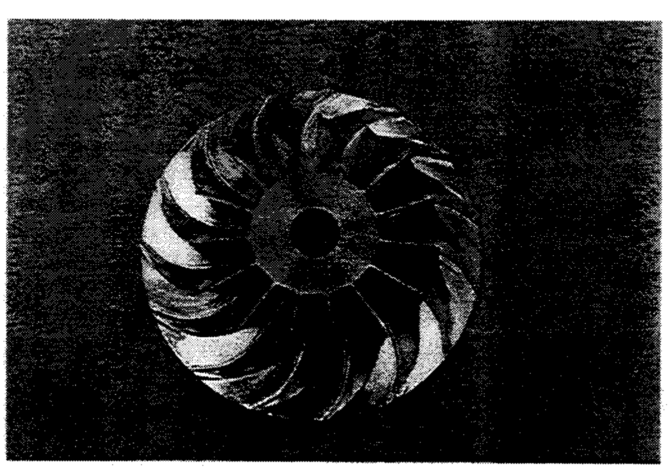

Fig. 10 A machined impeller with fifteen blades

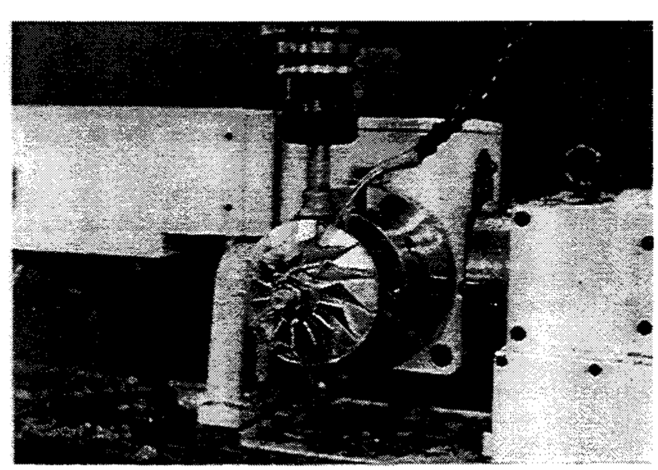

Fig. 11 Five-axis machining of an impeller with thirteen blades

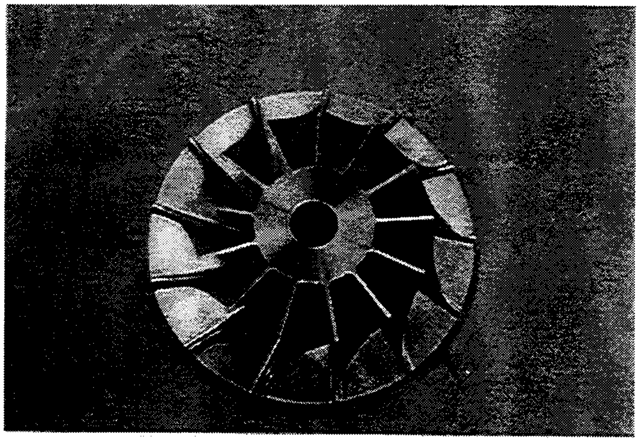

Fig. 12 A machined impeller with thirteen blades

DISCUSSION AND CONCLUSION

A simple and reliable procedure that can be applied to generate collision-free tool paths for five-axis machining of parts with complex shapes is developed. Regardless of the type of surfaces on a workpiece, only CC points are needed in the process of checking. As has been demonstrated by practical application examples, the feasibility and versatility of the approach is successfully verified. Though the procedure is illustrated by a popular type of a five-axis machining center, the approach to its implementation does not depend on the particular choice of hardware.

In this article, only the type of cylindrical ball-end cutters is handled in algorithms. For machining general turbomachinery components, different shapes of cutters may be also used and it is well worth making the effort to include them in the procedure. Also, the choice of a tilting angle from the feasible range of cutter-axis for maximum material-removal rate is being observed.

ACKNOWLEDGMENTS

This study is being supported by the National Science Council of Taiwan under grants of NSC 84-2212-E-110-005 and NSC 85-2622-E-110-007. The authors are grateful to Yi Tay Liu who developed the algorithm to produce geometric data from the preliminary design of impellers.

REFERENCES

Choi, B. K. and Jun, C. S., 1989, "Ball-end cutter interference avoidance in NC machining of sculptured surfaces," Computer-Aided Design, Vol. 21, No. 6, pp. 371-378.

Choi, B. K. 1991, Surface Modeling for CAD/CAM, Elsevier, Amsterdam, Netherlands.

Choi, B. K., Park, J. W., and Jun, C. S., 1993, "Cutter-location data optimization in 5-axis surface machining," Computer-Aided Design, Vol. 25, No. 6, pp. 377-386.

Faux, I. D. and Pratt, M. J., 1979, Computational Geometry for Design and Manufacture, Ellis Horwood Limited.

Hwang, J. S., 1992, "Interference-free tool-path generation in the NC machining of parametric compound surfaces," Computer-Aided Design, Vol. 24, No. 12, pp. 667-676.

Jerard, B., Drysdale, R. L., and Magewick, J., 1989, "Methods for Detecting Errors in Numerically Controlled Machining of Sculptured Surfaces," IEEE Computer Graphics & Applications, January, pp. 26-39.

Kim, B. H. and Chu, C. N., 1994, "Effect of cutter mark on surface roughness and scallop height in sculptured surface machining," Computer-Aided Design, Vol. 26, No. 3, pp. 179-188.

Lee, Y. S., 1993, Automatic Planning and Programming for Five-axis Sculptured Surface Machining, PhD Thesis, Purdue University.

Li, S. X. and Jerard, R. B., 1994, "5-axis machining of sculptured surfaces with a flat-end cutter," Computer-Aided Design, Vol. 26, No. 3, pp.165-178.

Loney, G. C. and Ozsoy, T. M., 1987, "NC machining of free form surfaces," Computer-Aided Design, Vol. 19, No. 2, pp.85-90.

Oliver, J. H., Wysocki, D. A., and Goodman E. D., 1993, "Gouge Detection Algorithms for Sculptured Surface NC Generation," Trans. ASME Journal of Engineering Industry, Vol. 115, pp. 139-144.

Rogers, D. F. and Adams, J. A., 1990, Mathematical Elements for Computer Graphics, 2nd Edition, McGraw-Hill Inc.

Smith, D. J. L. and Merryweather, H., 1973, "The Use of Analytic Surfaces for the Design of Centrifugal Impellers by Computer Graphics,' International Journal for Numerical Methods in Engineering, Vol. 7, pp. 137-154.

Suresh, K. and Yang, D. C. H, 1994, "Constant Scallop-height Machining of Free-form Surfaces," Trans. ASME Journal of Engineering Industry, Vol. 116, pp. 253-259.

Tsay, D. M. and Hwang, G. S., 1994, "The Profile Determination and Machining of Camoids with Oscillating Spherical Followers," Trans. ASME Journal of Engineering Industry, Vol. 116, pp. 355-362.

Takeuchi, Y. and Takahiro, W, 1992, "Generation of 5-Axis Control Collision-Free Tool Path and Postprecessing for NC Data," Annals of the CIRP, Vol. 41/1, pp. 539-542.

Takeuchi, Y. and Idemura, T, 1991, "5-Axis Control Machining and Grinding Based on Solid Model," Annals of the CIRP, Vol. 40/1, pp. 455-458.

Tseng Y. and Joshi S., 1991, "Determining feasible tool-approach directions for machining Bezier curves and surfaces," Computer-Aided Design, Vol. 23, N0. 5, pp. 36-379

Vickers, G. W. and Quan, K. W., 1989, "Ball-Mills Versus End-Mills for Curved Surface Machining," Trans. ASME Journal of Engineering Industry, Vol. 111, pp. 22-26.

Wang, W. P., 1990, "Three-Dimensional Collision Avoidance in Production Automation," Computers in Industry, Vol. 15, pp. 169-174.